Microchim Acta (2017) 184:4723–4729
DOI 10.1007/s00604-017-2499-2

ORIGINAL PAPER

Non-enzymatic amperometric hydrogen peroxide sensor using a glassy carbon electrode modified with gold nanoparticles deposited on CVD-grown graphene

Yawen Yuan[1] · Yiqun Zheng[2] · Jinglei Liu[2] · Hua Wang[2] · Shifeng Hou[2]

Received: 9 May 2017 / Accepted: 2 September 2017 / Published online: 20 September 2017

Abstract A glassy carbon electrode (GCE) was modified with gold nanoparticles (AuNPs) coated on monolayer graphene (AuNP/MG) by direct in situ sputtering of AuNPs on CVD-generated graphene. This process avoids complicated polymer transfer and polymer cleaning processes and affords AuNPs with a clean surface. The monolayer graphene is ductile and well dispersed. The clean surface of the AuNPs renders this sensor superior to GCEs modified with AuNPs on reduced graphene oxide in terms of the amperometric non-enzymatic determination of hydrogen peroxide. The detection limit is 10 nM (S/*N* = 3) at 0.55 V (vs. SCE), which is lower than that for similar methods, and the response time is as short as 2 s. Another attractive feature of the sensor is its feasibility for large-scale production via CVD and sputtering.

Keywords Chemical vapor deposition · Sputtering · Electrochemical sensing · Synergistic effect · Amperometry · Poly(methyl methacrylate)

Electronic supplementary material The online version of this article (https://doi.org/10.1007/s00604-017-2499-2) contains supplementary material, which is available to authorized users.

✉ Shifeng Hou
shifenghou@sdu.edu.cn

[1] School of Chemistry and Chemical Engineering, Shandong University, Jinan, Shandong 250100, People's Republic of China

[2] National Engineering and Technology Research Center for Colloidal Materials, Shandong University, Jinan, Shandong 250100, People's Republic of China

Introduction

Sensitive detection of hydrogen peroxide (H_2O_2) is of great significance in clinical, environmental, and food applications since H_2O_2 is an essential intermediate in the biomedical and chemical industries [1, 2]. Among the detection technologies available for H_2O_2, which are based on spectrofluorimetry [3], chemiluminescence [4], and electrochemistry [5], the electrochemical method is widely investigated because of its low cost, ease of operation, and good repeatability. Multifunctional modified electrodes were used to improve the electroactivity of H_2O_2, such as metals and metal oxides nanoparticles, carbon nanomaterials, polymer, dyes and their composites modified solid electrodes [6–14]. In this regard, graphene-supported noble metal nanoparticles have been widely investigated because graphene has potential applications in the electrochemical field and noble metal nanoparticles have outstanding catalytic ability for non-enzymatic H_2O_2 detection [15, 16].

Graphene has potential applications in electrochemistry because of its large specific surface area and remarkable mechanical and electrical properties [17–20]. The combination of graphene with noble metal nanoparticles results in two synergistic effects: (a) graphene acts as a support to immobilize and expose the active sites of the noble metal nanoparticles; (b) electron transport is effectively improved. In particular, graphene-supported gold nanoparticles composites have attracted intense research interest as gold nanoparticles have good biocompatibility and low charge transfer resistance, can be easily synthesized and functionalized [21–23].

However, graphene-supported gold nanoparticle sensors have some limitations. For example, exfoliation and reduction of graphite and graphene oxide degrade the quality of graphene. The residual oxygen functional groups decrease the electroconductivity of graphene. Moreover, the large

capacitance of powder graphene materials and the surfactant residual of gold nanoparticles render the sensor insensitive to low concentrations of H_2O_2 [24–28]. Hence, high-quality graphene-supported gold nanoparticles with a clean surface are necessary to optimize the catalytic performance. Chemical vapor deposition (CVD)-generated graphene has high quality, with well-preserved electronic and mechanical properties. However, complicated transfer process from the substrate hinders its application to electrochemical sensors [29, 30].

Herein, we optimized CVD-generated graphene-supported gold nanoparticles (AuNP/MG) to enhance the electrocatalytic activity of H_2O_2, with polymer-free transfer combined sputtering technology. The value of this work relies on the following aspects: i) monolayer graphene as a platform prevents stacking and agglomeration of gold nanoparticles, resulting in highly exposed active sites on the nanoparticles; ii) the sputtered gold nanoparticles have a clean surface without any surfactant, so that sensitivity of H_2O_2 detection is enhanced; iii) the free-standing AuNP/MG can be transferred without a polymer, avoiding the complicated transfer process and polymer residues. The morphology and features of AuNP/MG were determined, and the electrochemical performance was evaluated by cyclic voltammetry (CV) and amperometry for non-enzymatic H_2O_2 detection using actual samples. In addition, the direct formation of AuNP/MG free-standing films without polymer transfer may be suitable for large-scale production.

Experimental

Reagents

Cu foils were purchased from Alfa Aesar (25 μm thick, 99.8% metal basis, Shanghai, China, http://www.alfachina.cn/). H_2 and CH_4 gases with 99.99% purity were procured from Jinan Deyang Special Gas Company (Jinan, China, http://www.jndytq.com/). Reduced graphene oxide (rGO) powders were purchased from Leadernano Tech. L.L.C. (Jining, China, http://www.leadernano.com/) for comparison. Poly(methyl methacrylate) (PMMA) with an average molecular weight 97,000 was purchased from Sigma-Aldrich Co. L.L.C. (Shanghai, China, http://www.sigmaaldrich.com/). Ammonium persulfate ($(NH_4)_2S_2O_8$), hydrogen peroxide (H_2O_2, 30% mass fraction), chlorobenzene (C_6H_5Cl), acetone (CH_3COCH_3), acetic acid (CH_3COOH), sodium dihydrogen phosphate dihydrate ($NaH_2PO_4{\cdot}2H_2O$), and disodium hydrogen phosphate dihydrate ($Na_2HPO_4{\cdot}2H_2O$) were purchased from Sinopharm Chemical Regent Company (Shanghai, China, http://www.sinoreagent.com/). Aluminum oxide (Al_2O_3) powders with different diameters (300 nm and 50 nm) were obtained from Shanghai Chenhua Instrument Company (Shanghai, China, http://www.chinstr.com/). Phosphate buffer (0.1 $mol{\cdot}L^{-1}$) was prepared by using $NaH_2PO_4{\cdot}2H_2O$ and $Na_2HPO_4{\cdot}2H_2O$. PMMA solution with 5% mass fraction was obtained by dissolving PMMA in chlorobenzene. All reagents were of analytical grade and used without further purification. In all experiments, ultrapure water with a resistivity of 18.2 MΩ·cm was used.

Apparatus

CVD graphene was grown using G-CVD equipment from Xicheng Company (Xiamen, China, http://www.g-cvd.com/zh-cn/). Vacuum sputter equipment was obtained from Denton Vacuum Company (DESK V Cold Sputter, Moorestown, USA, http://www.dentonvacuum.com/). The gold target with 99.999% purity was purchased from GRIKIN Advanced Material Company (Beijing, China, http://www.grikin.com/). The spin coater (KW-4B) was purchased from Institute of Microelectronics of Chinese Academy of Sciences (Beijing, China, http://www.ime.cas.cn/). The electrochemical workstation (CHI-660C) with a standard three-electrode system (platinum plate, saturated calomel electrode, and glassy carbon electrode as the counter, reference, and working electrodes, respectively) was purchased from Shanghai ChenHua Instrument Company (Shanghai, China, http://www.chinstr.com/).

The morphology and structure of the samples were analyzed using transmission electron microscopy (TEM, JEOL, JEM-1011, Japan, http://www.jeolusa.com/), scanning electron microscopy (SEM, JSM-6700F, Japan, http://www.jeolusa.com/), X-ray photoelectron spectroscopy (XPS, ThermoFisher K-Alpha, USA, http://www.thermofisher.com/cn/zh/home.html/), and Raman spectroscopy (PHS-3C, Kyoto, Japan, http://www.horiba.com/).

Preparation of AuNP/MG

Monolayer graphene was prepared by the typical low-pressure chemical vapor deposition (LPCVD) method [31]. First, Cu foils were ultrasonically cleaned with acetone and acetic acid, and dried under N_2 at room temperature. Then, the Cu foils were loaded at the center of a quartz tube having a diameter of 5 cm and length of 1.5 m. The temperature of the tube was increased to 1030 °C under H_2 atmosphere in a furnace; then, CH_4 was introduced into the tube and the temperature was maintained at this level for 30 min. The H_2:CH_4 gas flow ratio was 4:1. Then, the furnace moved away and the samples cooled down to room temperature naturally.

Subsequently, the graphene-covered Cu foils were transferred to the vacuum sputter equipment. The sputtering power output was 30 W, and the sputtering time was 30 s. After sputtering, the samples were cut into 1 × 1 cm^2 pieces, and floated on the 0.2 $mol{\cdot}L^{-1}$ $(NH_4)_2S_2O_8$ solution overnight for etching of the Cu foil. Then, the samples (AuNP/MG) were washed with ultrapure water several times and temporarily stored by floatation on water.

Preparation of modified electrodes

A glassy carbon electrode (GCE) with 3 mm diameter was polished to mirror finish using Al_2O_3 suspension and ultrasonicated in ultrapure water and ethanol. The cleaned GCE was attached to the free-standing AuNP/MG in solution, ensuring close contact of graphene to the surface of the GCE. The modified electrodes were dried in air overnight so that the contact was stable for the following electrochemical testing; these electrodes were denoted as AuNP/MG/GCE.

The electrode denoted as AuNP/rGO/GCE was modified with rGO powder and gold nanoparticles. Removable GCE was used for the subsequent sputtering process. An ethanol dispersion of rGO (5 μL, 1 mg·mL^{-1}) was dropped onto clean surface of GCE, and dried naturally in air. Then, the GCE was removed, and the head was loaded onto the vacuum sputter equipment, sputtering as above mentions.

The CVD-generated graphene-modified glassy carbon electrode (MG/GCE) was prepared by PMMA-assisted transfer graphene on the surface of the GCE. The Cu foils covered with graphene were cut into 1 cm × 1 cm pieces and loaded on the spin coater. PMMA solution (5 μL, 5% mass fraction) was dropped and spin-coated on the surface of graphene on the Cu foils. Then the samples were heated on a heating plate at 120 °C. After curing, the samples were floated on $(NH_4)_2S_2O_8$ solution (0.2 mol·L^{-1}) to etch the Cu foils. The etched samples were washed with ultrapure water to remove residual $(NH_4)_2S_2O_8$ and stored in water. The clean surface of the GCE was used as the support for adhering to the sample so that the graphene surface was in contact with the GCE instead of PMMA. The MG/GCE was obtained after PMMA was removed with hot acetone.

Electrochemical measurements

20 mL of phosphate buffer was added to the homemade electrolytic cell, which contained a 25 mL beaker and a polytef cover plate, and N_2 was bubbled for 30 min to expel O_2. All the working voltages in this standard three-electrode system were measured against a saturated calomel electrode (SCE) at room temperature. CV measurements were carried out from - 0.1 V to 0.7 V (vs. SCE) to evaluate the electrochemical behavior of the modified electrodes. The amperometric i-t curve was measured for different concentrations of H_2O_2 injected at 0.55 V (vs. SCE), at regular intervals of 50 s. The amperometric response of H_2O_2 (5 μM) and added of 100 times concentration of dopamine, ascorbic acid, uric acid and glucose at 0.55 V (vs. SCE) was measured. In addition, H_2O_2 detection in a real sample (human serum) was achieved.

Results and discussion

Principle

The AuNP/MG obtained by CVD and sputtering is shown in Scheme 1. The AuNP/MG was stable in solution and on the electrode surface under ambient conditions. Van der Waals forces can account for the ultra-strong adhesion between graphene and the GCE surface after drying, and avoids graphene from scrolling [32]. The AuNP/MG/GCE sensor was fabricated by the adhering the AuNP/MG to the GCE surface without using any additive.

Choice of materials

The synergistic effect of the gold nanoparticles and CVD-generated graphene enhanced the electrochemical performance for H_2O_2 detection. CVD-generated graphene with a large specific surface area was an ideal platform for the dispersion of gold nanoparticles. The electronic and mechanical properties of graphene were preserved and were superior to those of similar graphene materials used in the field of electrochemistry. The good dispersion of gold nanoparticles with highly exposed active sites led to high catalytic efficiency for the detection of ultralow concentrations of H_2O_2.

Characterization of AuNP/MG

The morphology of the AuNP/MG was determined by scanning electron microscopy (SEM), as shown in Fig. 1. The gold

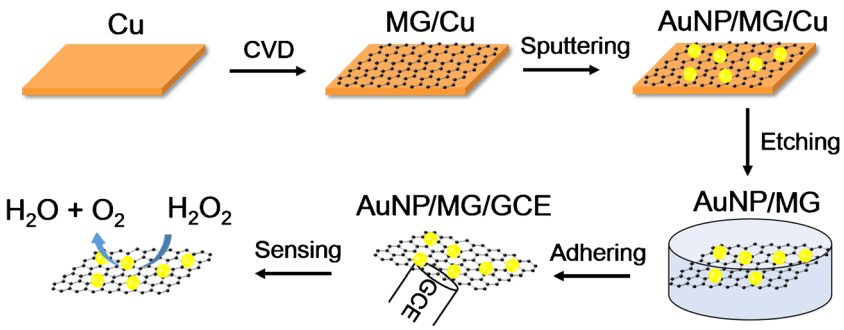

Scheme 1 Process of synthesize AuNP/MG/GCE and application in non-enzymatic H_2O_2 detection

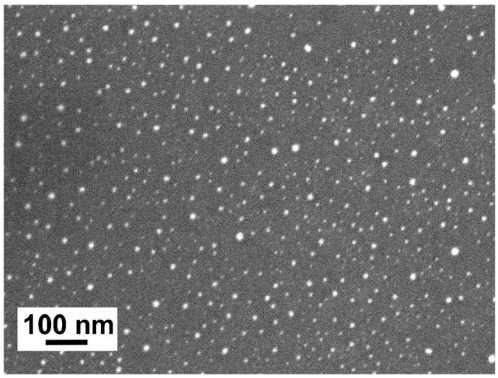

Fig. 1 SEM image of AuNP/MG on the surface of GCE (the bright particles are gold nanoparticles)

nanoparticles were loaded and homogeneously dispersed on the surface of graphene, confirming that free-transfer CVD graphene is a good platform to prevent agglomeration of the anchored gold nanoparticles and consequent surface blockage. The CVD-generated graphene showed good ductility and had some wrinkles caused by impurities (Fig. S1A). The AuNP/MG was fully covered and tiled without agglomeration on the surface of the GCE (Fig. S1B). The size distribution of the gold nanoparticles was investigated further by using a distribution histogram (Fig. S1C), and the average size of the nanoparticles was found to be 3 ± 0.125 nm (n = 300).

The CVD-generated graphene and AuNP/MG were characterized by Raman spectroscopy, as shown in Fig. 2. Graphene showed sharp G and 2D peaks at ~2645.7 cm^{-1} and ~1588.6 cm^{-1}, indicating good crystalline quality (blue curve). The intensity of the 2D peak indicated monolayer graphene, and the intensity of the D peaks located at ~1329.4 cm^{-1} was low, revealing that graphene primarily comprises sp^2 carbon [33, 34]. After sputtering the gold nanoparticles, the intensity of the 2D peak decreased slightly (red curve), indicating increased disorder in the AuNP/MG. The full width at half maximum (FWHM) of the G, 2D peaks

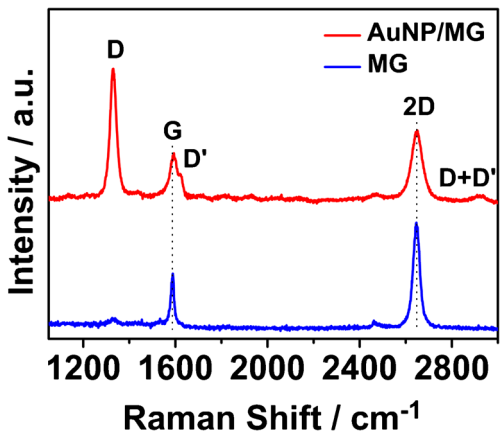

Fig. 2 Raman spectra of CVD-generated graphene (MG, blue curve) and AuNP/MG (red curve) load on copper foils

increased and the G peak showed a slight blue shift, which can be attributed to the tendency of graphene to form wrinkles. The peaks at 1621.4 cm^{-1} and 2940 cm^{-1} (D' and D + D' peak, respectively) indicated an increase in the number of defects caused by the sputtering deposition of the gold nanoparticles.

Electrochemical response of AuNP/MG/GCE

The electrochemical behavior of the AuNP/MG-modified glassy carbon electrode (AuNP/MG/GCE) toward H_2O_2 oxidation was investigated, as shown in Fig. 3. CV tests (Fig. 3a) were carried out in 20 mL phosphate buffer at the scan rate of 50 mV·s^{-1} from −0.1 to 0.7 V (vs. SCE). The capacitance of the AuNP/MG/GCE is similar to that of the MG/GCE and GCE but lower than that of the AuNP/rGO/GCE in the phosphate buffer without H_2O_2 (dashed line in Fig. 3a). When 25 μL of H_2O_2 (5 μM) was injected into the solution, the voltammograms of the MG/GCE (green solid line) and GCE (black solid line) showed no obvious peaks. However, the AuNP/MG/GCE (red solid line) yielded a distinct peak at 0.55 V (vs. SCE), which indicated good response of the AuNP/MG/GCE toward H_2O_2 detection. The mechanism of H_2O_2 oxidation has been reported previously [35]. The current peak at 0.55 V (vs. SCE) can be attributed to the electrochemical oxidation of H_2O_2, with intermediates finally convert to O_2. The gold nanoparticles catalyzed H_2O_2 and graphene as the platform can transport reaction electron and enhance the catalytic efficiency. The voltammogram of the AuNP/rGO/GCE (blue solid line) yielded no obvious peak, because of the stacked rGO layers.

The influence of scan rates on the redox peak current of AuNP/MG/GCE in the phosphate buffer containing 5 μM H_2O_2 is shown in Fig. 3b. The peak current at 0.55 V (vs. SCE) increased with increasing scan rate from 20 mV·s^{-1} to 200 mV·s^{-1} (intervals of 20 mV·s^{-1}). As depicted in the inset of Fig. 3b, the peak current shows a linear relationship with the square root of the scan rate, and the linear regression equation is I = 3.11E-06 × $\nu^{1/2}$–2.663E-07 (A, V·s^{-1}; correlation coefficient R^2 = 0.996; n = 10), which shows the dynamics control is diffusion process.

Amperometric determination of H_2O_2

The amperometric method was used to test the electrochemical detection performance of the AuNP/MG/GCE toward H_2O_2 in phosphate buffer. The classical current-time curve obtained by adding different concentrations of H_2O_2 solution into the stirring system at 0.55 V (vs. SCE) is shown in Fig. 4a. The curve showed good response toward H_2O_2, as indicated by the sharp step of current increase following the adding of H_2O_2. A response time (95% of the maximum response current value) within 2 s indicated fast response of

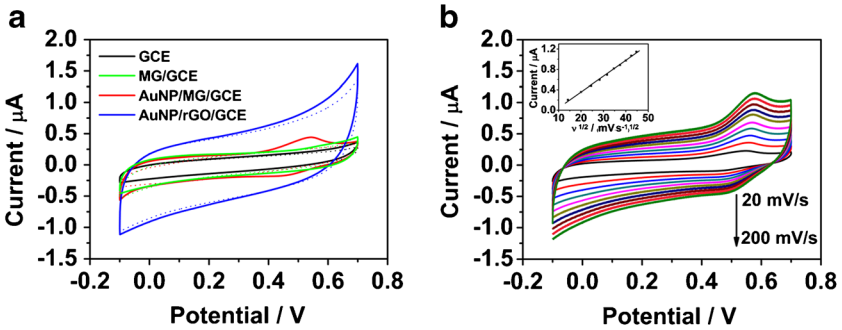

Fig. 3 **a** Cyclic voltammogram curves of: GCE (black curve), MG/GCE (green curve), AuNP/MG/GCE (red curve) and AuNP/rGO/GCE (blue curve) in phosphate buffer in the absence (dash line) and presence (solid line) of 5 μM H_2O_2 at scan rate of 50 mV·s^{-1}. **b** AuNP/MG/GCE in phosphate buffer containing 5 μM H_2O_2 at different scan rates with regular interval of 20 mV·s^{-1}, inset **b** was the plots of current value versus square root of scan rate at 0.55 V (vs. SCE)

the sensor. The curve of response current value versus concentration of H_2O_2 is shown in Fig. 4b. The current values mutated when higher concentrations of H_2O_2 were added, indicating the good sensitivity of the sensor toward ultralow concentrations of H_2O_2. The fitted curves showed good linear correlation with low and high concentrations of H_2O_2. The equalities were I = 0.0032 + 0.0215 × C (μA, μM, R^2 = 0.991, n = 14) and I = 0.1965 + 0.0045 × C (μA, μM, R^2 = 0.996, n = 11), respectively. The detection linear range ranged from 25 nM to 1.5 mM, with the detection limit of 10 nM at a signal-to-noise ratio of 3. The electrochemical sensitivity for ultralow concentrations of H_2O_2 was 0.3043 μA·μM^{-1}·cm^{-2}. Moreover, the current-time curve of the AuNP/MG/GCE for low concentrations of H_2O_2 (1 nM to 100 nM) is shown in Fig. S3A. The high hydrophobicity of the graphene surface and low capacitance of the monolayer graphene can account for the low initial current (in the order of 10^{-9} A) and good sensitivity for the detection of ultralow concentrations of H_2O_2.

The detection limit of the AuNP/MG/GCE for H_2O_2 was estimated to be 10 nM at a signal-to-noise ratio of 3, which was much lower than that of other graphene-supported gold nanoparticles, as shown in Table 1. The higher sensitivity can be attributed to the exposed active sites of the residue-free and well-dispersed gold nanoparticles on the ductile CVD monolayer graphene. In addition, the AuNP/MG was confirmed to show a small initial current, and no graphene layers were stacked to the encapsulate gold nanoparticles, which seemed to be the key to achieve better sensing performance than that of AuNP/rGO and other similar materials.

The selectivity of AuNP/MG/GCE for H_2O_2 detection was evaluated as shown in Fig. S3B. The amperometric response of H_2O_2 (5 μM) and the added 0.5 mM dopamine, ascorbic acid, uric acid and glucose at 0.55 V (vs. SCE) was measured. The result revealed the high selectivity of the AuNP/MG/GCE sensor from redox-active organic species.

Real sample detection and sensor stability

To evaluate the practical applicability of the AuNP/MG, the AuNP/MG/GCE sensor was used for testing human urine samples by the standard addition method. The results listed in Table S1 show the high recovery percentage and yield upon the addition of different concentrations of H_2O_2 to different

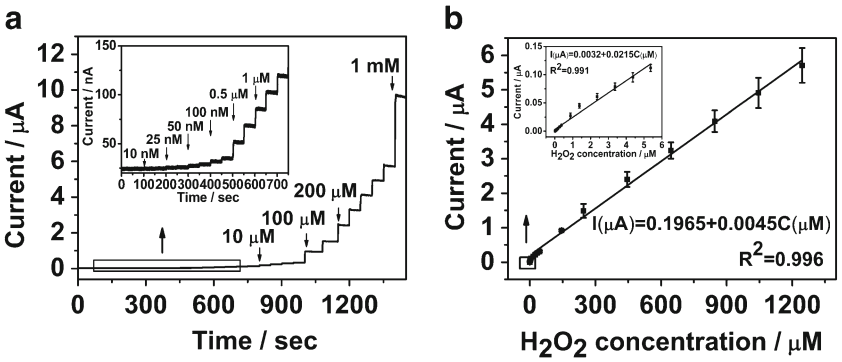

Fig. 4 **a** Amperometric curve of AuNP/MG/GCE with the injection of different concentration of H_2O_2 from 10 nM to 1 mM at 0.55 V (vs. SCE) with regular intervals of 50 s and inset **a** is the enlarged image of rectangle. **b** and inset **b** are plots of current value versus high and low concentrations of H_2O_2, respectively. The fitted equalities were I = 0.1965 + 0.0045 × C (μA, μM, R^2 = 0.996, n = 11) and I = 0.0032 + 0.0215 × C (μA, μM, R^2 = 0.991, n = 14) respectively

Table 1 The linear ranges and detection limits of AuNP/MG/GCE for H_2O_2 determination compared to previous reports

Modified electrodes	Linear range (μM)	Detection limit (μM)	Reference
Au/rGO	20–10,000	0.1	[21]
AuNPs/rGO	100–9000	1.5	[22]
GN/AuNPs [a]	0.5–50	0.22	[27]
GNPs/SGS [b]	20–1300	0.25	[36]
RGO/AuNPs	25–41,500	5	[37]
RGO/AuNPs	250–22,500	6.2	[38]
GR/AuNRs [c]	30–5000	10	[39]
AuNP/MG [d]	0.025–1500	0.01	This work

[a] Cationic polyelectrolyte functionalized graphene nanosheets/gold nanoparticles

[b] gold nanoparticles/sulfonated graphene sheets

[c] Graphene and gold nanorods composite

[d] Chemical vapor deposition monolayer graphene-supported gold nanoparticles

concentrations of spiked samples. The recovery percentage and yield were calculated from the current response value using the linear relationship in the inset of Fig. 4b. The relative standard deviations (RSD) for both parameters were less than 5%, indicating the excellent capability of the sensor to detect H_2O_2 in real samples. The sensor stored in a refrigerator at 4 °C for two weeks retained 94% of the initial current response, which indicated satisfactory long-range stability (Fig. S5). These results prove that the sensor has good stability and it can be used in practical applications for H_2O_2 detection.

Conclusion

In summary, composites of CVD-generated graphene-supported gold nanoparticles (AuNP/MG) successfully applied for the non-enzymatic detection of H_2O_2. Free-standing AuNP/MG was prepared by sputtering gold nanoparticles on monolayer graphene without the polymer transfer step. The high quality and free residues of graphene and gold nanoparticles with exposed catalytically active sites accounted for the enhanced catalyze performance of H_2O_2. The AuNP/MG/GCE sensor showed a low detection limit with rapid response, stability, and selectivity. Nevertheless, the major limitation is two equations of linear region of calibration plot, because the current value mutated upon the addition of higher concentrations of H_2O_2. In addition, the AuNP/MG showed promising application to real samples and large-scale preparation for H_2O_2 detection.

Acknowledgements The National Natural Science Foundation of China (Grant No. 21475076) and International S&T collaboration Program of China (No. 2015DFA50060) financially supported this work.

Compliance with ethical standards The author(s) declare that they have no competing interests.

References

1. Valko M, Izakovic M, Mazur M, Rhodes CJ, Telser J (2004) Role of oxygen radicals in DNA damage and cancer incidence. Mol Cell Biochem 266(1):37–56. https://doi.org/10.1023/b:mcbi.0000049134.69131.89
2. Rhee SG (2006) H_2O_2, a necessary evil for cell signaling. Science 312(5782):1882–1883. https://doi.org/10.1126/science.1130481
3. Liang L, Lan F, Li L, Su M, Ge S, Yu J, Liu H, Yan M (2016) Fluorescence "turn-on" determination of H_2O_2 using multilayer porous SiO_2/NGQDs and PdAu mimetics enzymatic/oxidative cleavage of single-stranded DNA. Biosens Bioelectron 82:204–211. https://doi.org/10.1016/j.bios.2016.03.076
4. Deng M, Xu SJ, Chen FN (2014) Enhanced chemiluminescence of the luminol-hydrogen peroxide system by BSA-stabilized au nanoclusters as a peroxidase mimic and its application. Anal Methods 6(9):3117–3123. https://doi.org/10.1039/C3AY42135J
5. Chen W, Cai S, Ren QQ, Wen W, Zhao YD (2012) Recent advances in electrochemical sensing for hydrogen peroxide: a review. Analyst 137(1):49–58. https://doi.org/10.1039/c1an15738h
6. Liu H, Weng L, Yang C (2017) A review on nanomaterial-based electrochemical sensors for H_2O_2, H_2S and NO inside cells or released by cells. Microchim Acta 184(5):1267–1283. https://doi.org/10.1007/s00604-017-2179-2
7. Wu Q, Sheng Q, Zheng J (2016) Nonenzymatic amperometric sensing of hydrogen peroxide using a glassy carbon electrode modified with a sandwich-structured nanocomposite consisting of silver nanoparticles, Co_3O_4 and reduced graphene oxide. Microchim Acta 183(6):1943–1951. https://doi.org/10.1007/s00604-016-1829-0
8. Lin Y, Chen X, Lin Y, Zhou Q, Tang D (2015) Non-enzymatic sensing of hydrogen peroxide using a glassy carbon electrode modified with a nanocomposite made from carbon nanotubes and molybdenum disulfide. Microchim Acta 182(9):1803–1809. https://doi.org/10.1007/s00604-015-1517-5
9. Li SJ, Du JM, Zhang JP, Zhang MJ, Chen J (2014) A glassy carbon electrode modified with a film composed of cobalt oxide nanoparticles and graphene for electrochemical sensing of H_2O_2. Microchim Acta 181(5):631–638. https://doi.org/10.1007/s00604-014-1164-2
10. Hsu SY, Lee CL (2017) Sonoelectrochemical exfoliation of highly oriented pyrolytic graphite for preparing defective few-layered graphene with promising activity for non-enzymatic H_2O_2 sensors. Microchim Acta. https://doi.org/10.1007/s00604-017-2297-x
11. Cui X, Wu S, Li Y, Wan G (2015) Sensing hydrogen peroxide using a glassy carbon electrode modified with in-situ electrodeposited platinum-gold bimetallic nanoclusters on a graphene surface.

Microchim Acta 182(1):265–272. https://doi.org/10.1007/s00604-014-1321-7
12. Zhou H, Gan X, Wang J, Zhu X, Li G (2005) Hemoglobin-based hydrogen peroxide biosensor tuned by the photovoltaic effect of Nano titanium dioxide. Anal Chem 77(18):6102–6104. https://doi.org/10.1021/ac050924a
13. Xu Y, Chen Y, Yang N, Sun L, Li G (2012) DNA-templated silver nanoclusters formation at gold electrode surface and its application to hydrogen peroxide detection. Chin J Chem 30(9):1962–1965. https://doi.org/10.1002/cjoc.201200267
14. Zhao J, Yan Y, Zhu L, Li X, Li G (2013) An amperometric biosensor for the detection of hydrogen peroxide released from human breast cancer cells. Biosens Bioelectron 41:815–819. https://doi.org/10.1016/j.bios.2012.10.019
15. Zhang R, Chen W (2017) Recent advances in graphene-based nanomaterials for fabricating electrochemical hydrogen peroxide sensors. Biosens Bioelectron 89:249–268. https://doi.org/10.1016/j.bios.2016.01.080
16. Chen S, Yuan R, Chai Y, Hu F (2013) Electrochemical sensing of hydrogen peroxide using metal nanoparticles: a review. Microchim Acta 180(1–2):15–32. https://doi.org/10.1007/s00604-012-0904-4
17. Geim AK, Novoselov KS (2007) The rise of graphene. Nat Mater 6(3):183–191. https://doi.org/10.1038/nmat1849
18. Pumera M (2010) Graphene-based nanomaterials and their electrochemistry. Chem Soc Rev 39(11):4146–4157. https://doi.org/10.1039/c002690p
19. Shao Y, Wang J, Wu H, Liu J, Aksay IA, Lin Y (2010) Graphene based electrochemical sensors and biosensors: a review. Electroanalysis 22(10):1027–1036. https://doi.org/10.1002/elan.200900571
20. Pei H, Zhu S, Yang M, Kong R, Zheng Y, Qu F (2015) Graphene oxide quantum dots@silver core-shell nanocrystals as turn-on fluorescent nanoprobe for ultrasensitive detection of prostate specific antigen. Biosens Bioelectron 74:909–914. https://doi.org/10.1016/j.bios.2015.07.056
21. Dhara K, Ramachandran T, Nair BG, Satheesh Babu TG (2016) Au nanoparticles decorated reduced graphene oxide for the fabrication of disposable nonenzymatic hydrogen peroxide sensor. J Electroanal Chem 764:64–70. https://doi.org/10.1016/j.jelechem.2016.01.011
22. Qin X, Li Q, Asiri AM, Al-Youbi AO, Sun X (2013) One-pot synthesis of au nanoparticles/reduced graphene oxide nanocomposites and their application for electrochemical H_2O_2, glucose, and hydrazine sensing. Gold Bull 47(1–2):3–8. https://doi.org/10.1007/s13404-013-0094-9
23. Luo J, Rasooly A, Wang L, Zeng K, Shen C, Qian P, Yang M, Qu F (2016) Fluorescent turn-on determination of the activity of peptidases using peptide templated gold nanoclusters. Microchim Acta 183(2):605–610. https://doi.org/10.1007/s00604-015-1683-5
24. Park S, Ruoff RS (2009) Chemical methods for the production of graphenes. Nat Nanotechnol 4(4):217–224. https://doi.org/10.1038/nnano.2009.58
25. Xia ZY, Pezzini S, Treossi E, Giambastiani G, Corticelli F, Morandi V, Zanelli A, Bellani V, Palermo V (2013) The exfoliation of graphene in liquids by electrochemical, chemical, and sonication-assisted techniques: a nanoscale study. Adv Funct Mater 23(37):4684–4693. https://doi.org/10.1002/adfm.201203686
26. Zhou M, Zhai Y, Dong S (2009) Electrochemical sensing and biosensing platform based on chemically reduced graphene oxide. Anal Chem 81(14):5603–5613. https://doi.org/10.1021/ac900136z
27. Fang Y, Guo S, Zhu C, Zhai Y, Wang E (2010) Self-assembly of cationic polyelectrolyte-functionalized graphene Nanosheets and gold nanoparticles: a two-dimensional Heterostructure for hydrogen peroxide sensing. Langmuir 26(13):11277–11282. https://doi.org/10.1021/la100575g
28. Hu J, Li F, Wang K, Han D, Zhang Q, Yuan J, Niu L (2012) One-step synthesis of graphene-AuNPs by HMTA and the electrocatalytical application for O_2 and H_2O_2. Talanta 93:345–349. https://doi.org/10.1016/j.talanta.2012.02.050
29. Liang X, Sperling BA, Calizo I, Cheng G, Hacker CA, Zhang Q, Obeng Y, Yan K, Peng H, Li Q, Zhu X, Yuan H, Hight Walker AR, Liu Z, Peng LM, Richter CA (2011) Toward clean and crackless transfer of graphene. ACS Nano 5(11):9144–9153. https://doi.org/10.1021/nn203377t
30. Yuan Y, Zhang F, Wang H, Liu J, Zheng Y, Hou S (2017) Chemical vapor deposition graphene combined with Pt nanoparticles applied in non-enzymatic sensing of ultralow concentrations of hydrogen peroxide. RSC Adv 7(49):30542–30547. https://doi.org/10.1039/c7ra05243j
31. Li X, Cai W, An J, Kim S, Nah J, Yang D, Piner R, Velamakanni A, Jung I, Tutuc E, Banerjee SK, Colombo L, Ruoff RS (2009) Large-area synthesis of high-quality and uniform graphene films on copper foils. Science 324(5932):1312–1314. https://doi.org/10.1126/science.1171245
32. Booth TJ, Blake P, Nair RR, Jiang D, Hill EW, Bangert U, Bleloch A, Gass M, Novoselov KS, Katsnelson MI, Geim AK (2008) Macroscopic graphene membranes and their extraordinary stiffness. Nano Lett 8(8):2442–2446. https://doi.org/10.1021/nl801412y
33. Malard LM, Pimenta MA, Dresselhaus G, Dresselhaus MS (2009) Raman spectroscopy in graphene. Phys Rep 473(5–6):51–87. https://doi.org/10.1016/j.physrep.2009.02.003
34. Ferrari AC, Basko DM (2013) Raman spectroscopy as a versatile tool for studying the properties of graphene. Nat Nanotechnol 8(4):235–246. https://doi.org/10.1038/nnano.2013.46
35. Miah MR, Ohsaka T (2006) Cathodic detection of H_2O_2 using iodide-modified gold electrode in alkaline media. Anal Chem 78(4):1200–1205. https://doi.org/10.1021/ac0515935
36. Li SJ, Shi YF, Liu L, Song LX, Pang H, Du JM (2012) Electrostatic self-assembly for preparation of sulfonated graphene/gold nanoparticle hybrids and their application for hydrogen peroxide sensing. Electrochim Acta 85:628–635. https://doi.org/10.1016/j.electacta.2012.08.118
37. Bai X, Shiu KK (2014) Investigation of the optimal weight contents of reduced graphene oxide–gold nanoparticles composites and theirs application in electrochemical biosensors. J Electroanal Chem 720-721:84–91. https://doi.org/10.1016/j.jelechem.2014.03.031
38. Zhang P, Zhang X, Zhang S, Lu X, Li Q, Su Z, Wei G (2013) One-pot green synthesis, characterizations, and biosensor application of self-assembled reduced graphene oxide–gold nanoparticle hybrid membranes. J Mater Chem B 1(47):6525. https://doi.org/10.1039/c3tb21270j
39. Pang P, Yang Z, Xiao S, Xie J, Zhang Y, Gao Y (2014) Nonenzymatic amperometric determination of hydrogen peroxide by graphene and gold nanorods nanocomposite modified electrode. J Electroanal Chem 727:27–33. https://doi.org/10.1016/j.jelechem.2014.05.028